FOVLC: FOVEATION BASED DATA HIDING IN DISPLAY TRANSMITTERS FOR VISIBLE LIGHT COMMUNICATIONS

A Thesis

by

Özgür Yıldız

Submitted to the
Graduate School of Sciences and Engineering
In Partial Fulfillment of the Requirements for
the Degree of

Master of Science

in the
Department of Electrical and Electronics Engineering

Özyeğin University
May 2018

FOVLC: FOVEATION BASED DATA HIDING IN DISPLAY TRANSMITTERS FOR VISIBLE LIGHT COMMUNICATIONS

Approved by:

Asst. Professor Burhan Gülbahar, Advisor
Department of Electrical and Electronics Engineering
Özyeğin University

Asst. Professor Reyat Yılmaz
Department of Electrical and Electronics Engineering
Dokuz Eyül University

Asst. Professor Ahmet Tekin
Department of Electrical and Electronics Engineering
Özyeğin University

Date Approved: 18 May 2018

To my Family and Friends...

ABSTRACT

Visible light communications is an emerging architecture with unlicensed and huge bandwidth resources, security, and experimental implementations and standardization efforts. Display based transmitter and camera based receiver architectures are alternatives for device-to-device (D2D) and local area networking (LAN) systems by utilizing widely available TV, tablet and mobile phone screens as transmitters while commercially available cameras as receivers. Current architectures utilizing data hiding and unobtrusive steganography methods promise data transmission without user distraction on the screen. However, current architectures have challenges with the limited capability of data hiding in translucency or color shift based methods of hiding by uniformly distributing modulation throughout the screen and keeping eye discomfort at an acceptable level. In this article, foveation property of human visual system is utilized to define a novel modulation method denoted by FoVLC which adaptively improves data hiding capability throughout the screen based on the current eye focus point of viewer. Theoretical modelling of modulation and demodulation mechanisms hiding data in color shifts of pixel blocks is provided while experiments are performed for both FoVLC method and uniform data hiding denoted as conventional method. Experimental tests for the simple design as a proof of concept decreases average bit error rate (BER) to approximately half of the value obtained with the conventional method without user distraction while promising future efforts for optimizing block sizes and utilizing error correction codes.

ÖZETÇE

Görünür Işıkla Haberleşme (VLC) son zamanlarda yoğun olarak güvenlik ve standartlaştırma üzerine deneysel çalışmaları yapılan, lisansız yüksek bant genişliğine sahip kablosuz haberleşme teknolojisidir. Günlük hayatta sıkça karşılaştığımız televizyon, tablet ve mobil telefon ekranlarını verici, kameraları ise alıcı olarak kullanarak kurulabilecek bir VLC mimarisi, günümüzde kullanılan cihazdan cihaza iletişim (D2D) ve yerel ağ bağlantısı (LAN) sistemleri için iyi bir alternatif olacaktr. VLC ve görüntüleme işleminin birlikte yapılabilmesi için günümüz teknolojileri, resim üzerindeki bilgi gizleme işlemini insan gözünün göremeyeceği ve alıcı kameranın algılayabileceği şekilde optimize etmektedirler. Fakat bu teknolojiler, insan gözünün resim üzerindeki renk ve luminans değişikliklerine olan hassasiyeti sebebiyle sınırlı bir şekilde yapılan bilgi gizleme işleminden dolayı hala yüksek bit hata oranları (BER) ve düşük kanal kapasitesi gibi sıkıntılar içermektedir. Bu çalşmada özgün bir bilgi modulasyon tekniği olan, insan gözünün görüntüleme ekranı üzerinde odaklandığı nokta ve odaklanmadığı bölgelerdeki görüş kaybına uyarlanabilir bir şekilde bilgi gizleme tekniğini geliştirmeyi amaçlayan FoVLC ele alınmıştır. İnsan görüş sisteminin (HVS) görüntüleme ekranı üzerinde odaklanmadığı bölgelerdeki görüş kaybı matematiksel olarak modellenerek, FoVLC ve "geleneksel metot" olarak adlandırılan resmin her bölgesine eşit büyüklükte bilgi gizleyen sistem için renk kaydırma yöntemi ile modülasyon ve demodülasyon tekniği anlatılmıştır. Yapılan karşılaştırmalı testler sonucunda önerilen sistemin (FoVLC) geleneksek method'a göre belirtilen koşullar altında bit hata oranını (BER) ortalama yarı yarıya indirdiği ve aynı zamanda insan gözü tarafından daha zor algılandığı gözlenmiştir.

ACKNOWLEDGEMENTS

First of all, I would like to thank my advisor Asst. Professor Burhan Gülbahar for his continuous guidance and support. I'm also thankful to my team mates and supervisor for their understanding during my master thesis.

I am grateful to my colleague, Mr. M. Salih Kılıç for his ideas and invaluable support during the article preparation studies.

I would like to thank my company VESTEL for providing me an opportunity to get a Master Degree.

I really appreciate for the suggestions and complaints directed by Asst. Professor Reyat Yılmaz and Asst. Professor Ahmet Tekin.

Finally I'm really thankful to all my family.

TABLE OF CONTENTS

LIST OF TABLES

LIST OF FIGURES

Table 1: List of abbreviations

FoVLC	Foveation Based Data Hiding in Display Transmitter
GMB	Grid Message Block
VLC	Visible Light Communication
RF	Radio Frequency
MIMO	Multiple Input Multiple Output
LEA	Led Emitting Array
LED	Light Emitting Diode
CFL	Compact Fluorescent Lamp
BER	Bit Error Rate
LOS	Line of sight
5G	Fifth Generation
HVS	Human Visual System
RGC	Retinal Ganglion Cell
STB	Set Top Box
DS	Digital Signage
FPS	Frame Per Second

CHAPTER I

INTRODUCTION

Visible light communications (VLC) is a significant alternative to radio frequency (RF) communications with high and unlicensed bandwidth reaching THz, low cost system utilizing available light sources and display screens as transmitters, security with line-of-sight (LOS) and local physical channels and standardization efforts promising utilization in 5G platforms [1–3]. With the development and popularity of camera and display technologies, a different form of visible light communication between display screen and camera has emerged by the utilization of sensitivity differences between human eye and camera [5–10, 20]. Recent studies using data hiding or steganography based methods provide eye comfort by modulating data in the image on the display screen without distracting user such as in color or translucency changes uniformly throughout the screen. However, human visual system (HVS) has a special foveation property where the distraction outside the eye focus point gets smaller in a way that data hiding capacity can be improved significantly in an adaptive manner [4]. In this study, foveation property is utilized to design and implement a novel modulation method denoted by FoVLC by adaptively increasing color shifts in areas out of focus of the viewer to decrease bit error rate (BER) of data transmission. The method uniformly performing data hiding throughout the screen by using color shifts in pixels is denoted by *conventional method*. Proposed proof of concept design achieves to decrease BER compared with the conventional method for simple experimental set-up with TV based transmitter and commercial camera based receiver architecture. Furthermore, it provides better data invisibility compared with conventional method. Optimization of the block size and error correction coding with

respect to the properties of VLC channel and ambient interference is left as a future work. In this chapter, motivations behind this thesis, contributions and organization are described.

1.1 Motivations

Developed hand-held cameras and display devices gain more importance in our daily life over time. Electronic devices such as TV, digital signage units, set-top box (STB), blu ray player and mobile phones, handle complex tasks by cooperating with each other. Therefore, necessity of efficient short range wireless data communication system is inevitable. Today, generally radio wave based communication method such as WiFi and Bluetooth are used for the task. Radio wave signals are not directional and can get through the walls, however, the main disadvantage of this technology is handshaking procedure that makes it impractical. For example, user has to match transmitter and receiver devices to each other by manually selecting the device and entering the password. In addition, when a lot of user try to connect to the same router, each receiver gets a decreased bandwidth service. If communicating devices had display screen-camera pair such as TV and mobile phone, communication in visible light spectrum would be more healthy and efficient as an alternative in the field of wireless communications. Methods motivated by these facts, simply follow these steps: the data is embedded into regular images in an invisible manner, transmitter display screen shows the image with hidden data and the receiver camera captures the image and analyses to extract the data. If the process continues for all video frames in real time, optical channel for transmitting massive information data is created. However communication should be implemented in parallel to the main task of video display screen and this simultaneous process provides both energy efficiency and communications capability.

In [20], the data transmission speed up to 360 Kbit/s is reached. In [34, 35, 38],

the display detection methods, the angle between receiver camera and transmitter display and communication capacity under perspective distortions are analysed respectively. However HVS related subjects are quite kept out of research area. Medical research about human eye has always been an inspiration source for information and communication technologies. Since the most important receiver of display technology is human eye, understanding how human physcovisual model works is the key for the optimization of display related systems. Beside that, since the display screen size is becoming larger each year, the applications using foveated approaches will be more favourable. With this motivation, there are a lot of studies about foveated video compression [14, 16], image processing [17], virtual reality related subjects [18]. There are detailed medical research result [19, 29] which fussily investigate the distribution of retinal ganglion cells that decide the upper limit of human visual ability about spatial resolution according to increasing eccentricity. In this article, foveation property of human visual system (HVS) is utilized to define a novel display transmitter-based VLC modulation method denoted by FoVLC modulating color changes in pixels in an adaptive manner based on the current focus of the viewer. To realize the phenomenon, spatially uniform color shift based screen camera communication system [10] has been implemented in MATLAB in a simplified manner. We have analysed the effects of performance parameters for the designed system utilizing foveation property of HVS. Therefore, our general modeling promises utilization in other areas of digital image processing and optical communications subjects. Throughout the thesis, we have compared our method denoted by "FoVLC" with the state of the art denoted by "conventional".

1.2 Contributions of the Thesis

We have performed the following publications and patent applications during the thesis study:

1. B. Gulbahar, O. Yildiz, "Foveation based unobtrusive and stenographic ultra-high rate visible light communication system and method," *EPO Patent Application*, PCT/EP2016/081998, January 2017.

2. O. Yildiz, B. Gulbahar, "FoVLC: Foveation based data hiding in display transmitters for visible light communications," to appear in *Proceedings of The 14th IEEE International Wireless Communications and Mobile Computing Conference (IWCMC 2018), WON Symposium*, Limassol, Cyprus, June 2018.

In this thesis, the contributions, achieved for the first time, are listed as follows:

- Theoretical modeling and experimental tests (including BER performance and data invisibility tests with people subjects) of a novel VLC display based modulation and camera receiver based demodulation method denoted by FoVLC by utilizing foveation property of HVS.

- Improving conventional VLC data hiding methods utilizing color shift property on display screens by exploiting foveation property of HVS with experimental verification for a simple proof of concept system design.

- Analysing the effect of display screen and camera properties (i.e. white point, white balance) to the communication accuracy.

- Open issues to optimize FoVLC design.

1.3 Organization

In Chapter 2, human visual system is described. The basics of visible light communication is introduced in Chapter 3 while the device to device communication types are discussed in Chapter 4. In Chapter 5, screen camera communication methods using foveation based data modulation and uniform data modulation are compared

by numerical simulations and experimental results. In Chapter 6 challenges and open issues are presented while in Chapter 7, conclusion is given.

CHAPTER II

HUMAN VISUAL SYSTEM

In this chapter, human visual system is modelled in detail while mathematical model of human visual spatial resolution on a display based VLC transmitter device is presented in Chapter 5.

2.1 Introduction

The eye is a marvel by having the properties of great light adaptivity, wide field of view, high resolution and huge contrast and color range that any visual technology still could not achieve but it is not faultless. Moreover, the scene we see is not the image that is captured by our eye but the reconstruction of frames captured by both of eyes. Thus understanding the human eye structure, visual sense of human brain and human visual properties has vital importance for improving the performance of the studies.

2.2 Human Eye Structure

The reflected or emitted light by objects enters from the cornea, directed into the eyeball by the lens and falls onto the retinal periphery as shown in Fig 1. In the retina, the light rays are converted into visual signals, reorganized and transmitted to the brain by photo receptors, retinal ganglion cells and optical nerve, respectively. Reconstruction of image is done in visual cortex (an area in brain) with the signals gathered from both eyes. The whole system providing vision, is referred to as human visual system (HVS) [28]. According to the flowchart of the system, the seeing activity starts with the projection of light onto the retina. Retina is a complex structure and has mainly two layers; outer layer includes photo receptors (rods and cones) and inner

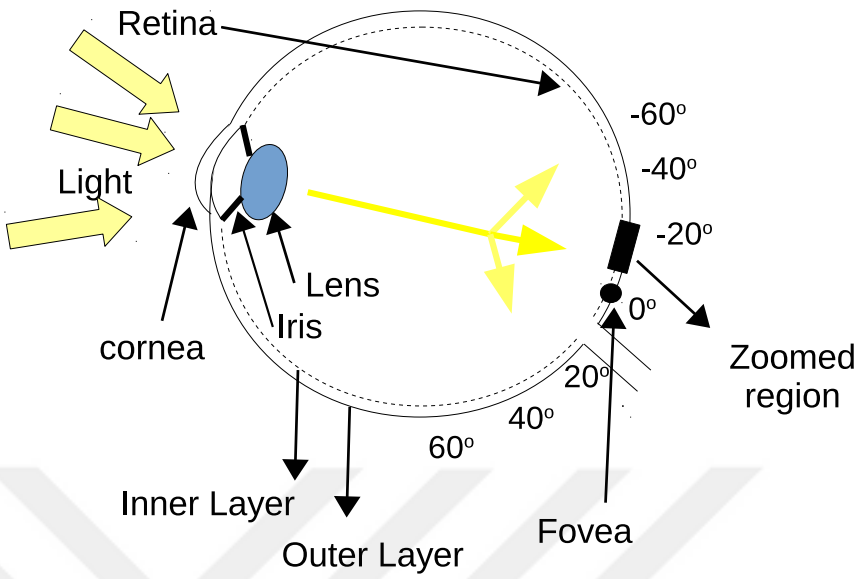

Figure 1: Simplified structure of eye. The iris controls the diameter of lens for adapting eye against ambient light. The incident light rays are reflected from the outer layer of retina and converted to visual signals by the retinal elements.

layer includes ganglion cells as shown in Fig. 2.

2.2.1 Photo Receptors

Rods and cones are the initial light sampling retinal elements existing densely in foveal region while the density decreases in peripheral region. The density of photo receptors is one of the effective factors on determining visual acuity and is shown in Fig 4. The cones operate in daylight conditions and provide the perception of color details of the field of view while the rods function in low light environment which only provide the perception of shade of gray. Daylight vision which is mostly provided by cones is referred as photopic while the lowlight vision is called scotopic [29].

2.2.2 Retinal Ganglion Cell (RGC)

Since the proposed method encodes the data by modulating color properties of images shown on display screen, this study focuses on photopic vision. The main limitation on the spatial resolution of human visual system is the spatial sampling by retinal

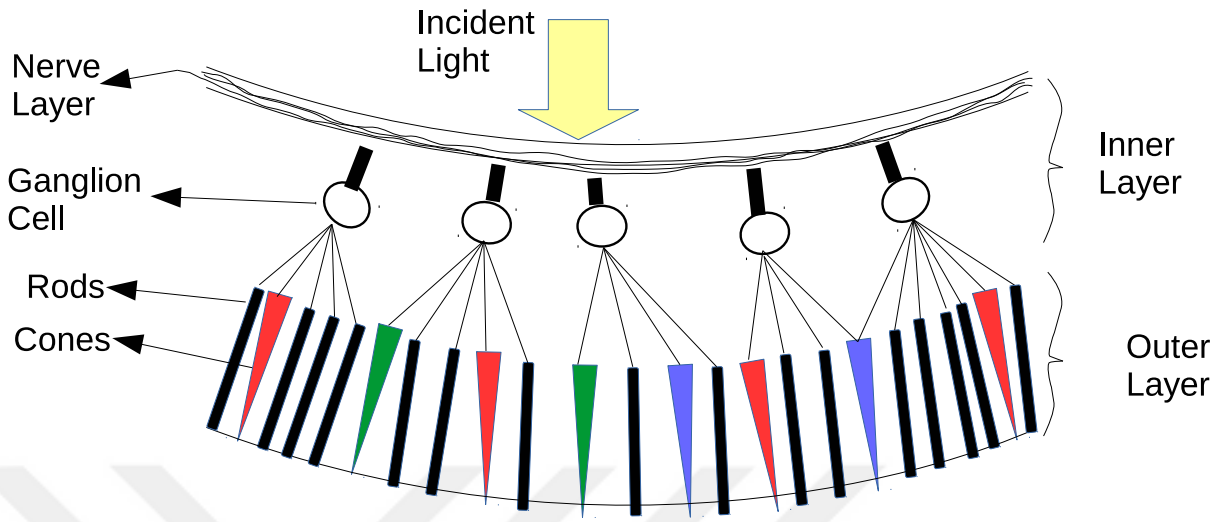

Figure 2: The cross-section of the zoomed region of the retinal structure shown in Fig. 1. It is adapted from [27].

neurons beyond optical blur. Visual signals are sampled first by the cones and then resampled by the retinal ganglion cells, whose properties limit the transfer of the signals to the brain since they are the final cells before the optic nerve. The most prevalent type of these RGCs is the midget RGC (mRGC) and they sample the cones one to one in fovea region whereas they sample multiple cones in peripheral region as shown in Fig 4. Therefore, the spatial resolution of human vision is bounded by the density of midget retinal ganglion cell receptive fields (mRGCfs) [19]. The density of mRGCf is shown in Fig. 3.

2.3 Visual Fields

The eye ball is like a three dimensional spherical organ and separated by four principal meridians which are originated from the visual center. The closest meridian of both eye to the nose is called nasal meridian while the horizontally outer meridians are called temporal meridians therefore horizontal principal meridians of both eye are symmetric according to the nose. The meridians reclining along the vertical direction are called superior and inferior meridians respectively. Similarly, visual fields are

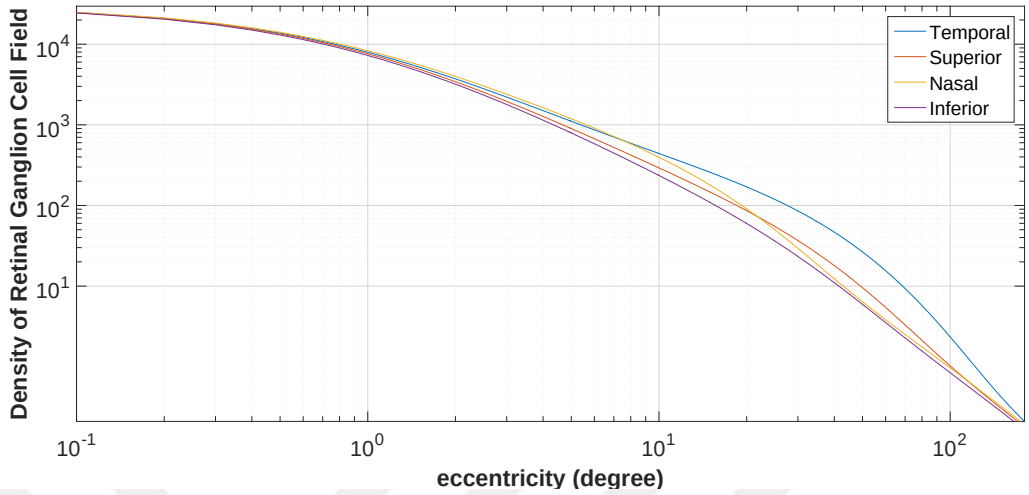

Figure 3: The density of mRGCf against eccentricity over four principal retinal meridians. It is adapted from [19].

separated according to these principal meridians. The left and right visual fields of each eye are divided by vertical line while the superior and inferior visual fields of each eye are divided by horizontal line in space [32]. The simplified illustration of principal meridians and visual fields of eye is depicted in Fig. 5.

2.4 Vision

The visual ability has dramatic changes as the distance increases from the point of fixation which is shown in Fig. 5. It is the point where eye gaze is focused on. HVS properties differs according to the environmental condition, vision fields and the distance from the point of fixation.

2.4.1 Central Vision

The central vision refers to the area around the point of fixation as shown in Fig. 5 so the light rays belonging to the central vision are perceived in the foveal region of the retina. The eye can detect even fine detail over central visual field. The basic properties of central vision are;

- Under high illumination (photopic vision), central vision performs best.
- Mostly benefits from cones which are densely located in the fovea.
- Almost one to one data transmission between cones and RGCs in the fovea, provides highest color sensitivity.

2.4.2 Peripheral Vision

The peripheral vision refers to the area out of central vision. The light rays belong to the peripheral vision are processed out of the foveal region of retina. The basic properties of peripheral vision are;

- It performs better under low light conditions (scotopic vision).
- It mostly benefits from rods which provide the perception of dim light variation in dark.
- It is less sensitive to the color changes.
- It has less spatial resolution.

2.4.3 Temporal Vision

The perception of HVS is too slow for fast color and luminance changes. If an object's intensity changes from dark to bright, it appears as a gray object above a certain frequency which is called flicker fusion threshold or flicker fusion rate [30]. Below this frequency our eye can separate the intensity or perceive the flicker. The basic properties of temporal vision are;

- Peripheral vision can detect higher flicker frequency than central vision.
- In a bright ambient light condition HVS has a better temporal perception.
- In a bright light condition, peripheral vision can detect up to 70 Hz flicker rate while a few Hz is enough in central vision for a steady impression [30].

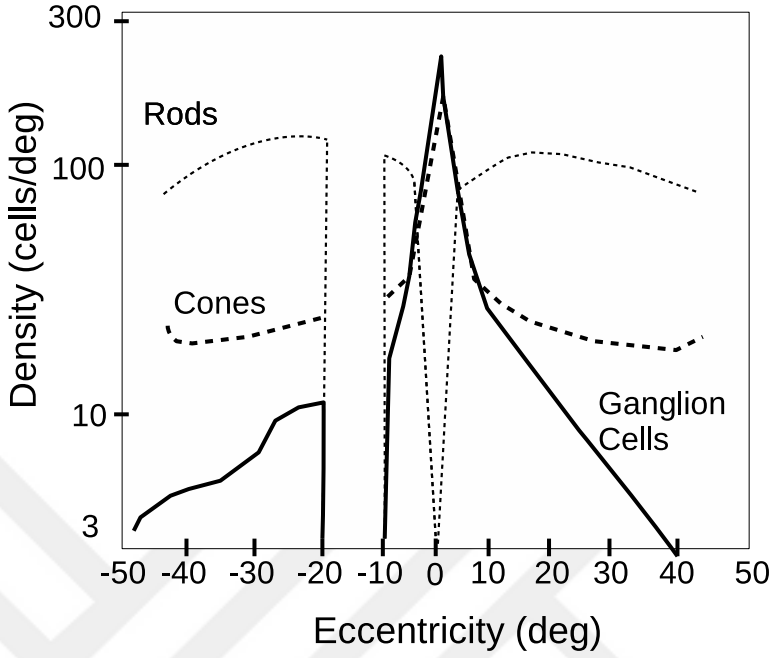

Figure 4: The figure depicts the density of rodes, cones and ganglion cells against increasing eccentricity over the retinal field. Adapted from [31].

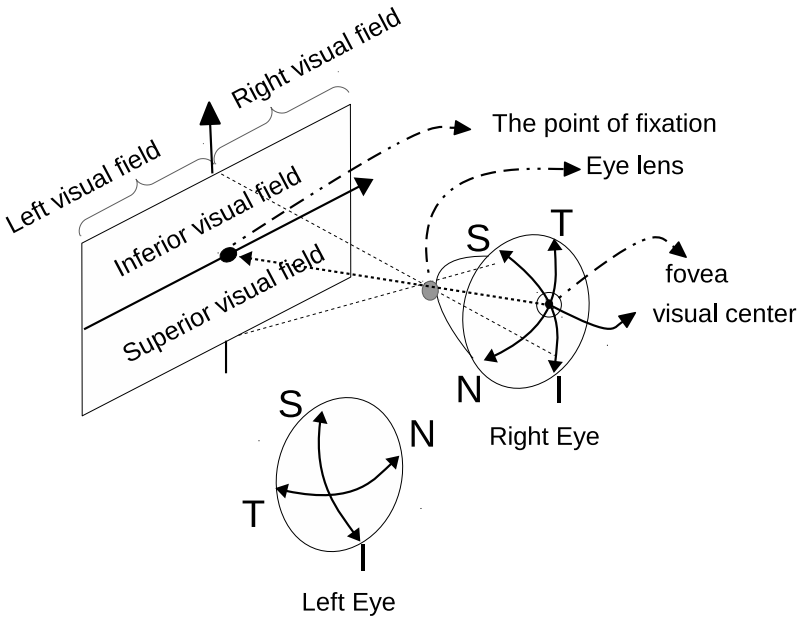

Figure 5: Visual fields and four principal retinal meridians originated from visual center along the retina of the eye. Note that fovea is an area not a point. N, S, T and I refers Nasal, Superior, Temporal and Inferior, respectively.

CHAPTER III

THE BASICS OF VISIBLE LIGHT COMMUNICATION

3.1 Overview

Visible light is a type of electromagnetic energy and visible light communication (VLC) is becoming the most popular alternative or auxiliary technique for the next generation wireless communication due to offering solutions for the cost, security, data rate, health hazard subjects of the existing RF communication technology. The VLC system uses visible light for communication that allocates the frequency spectrum from 400 THz to 790 Thz with its colour distribution as shown in Fig. 6.

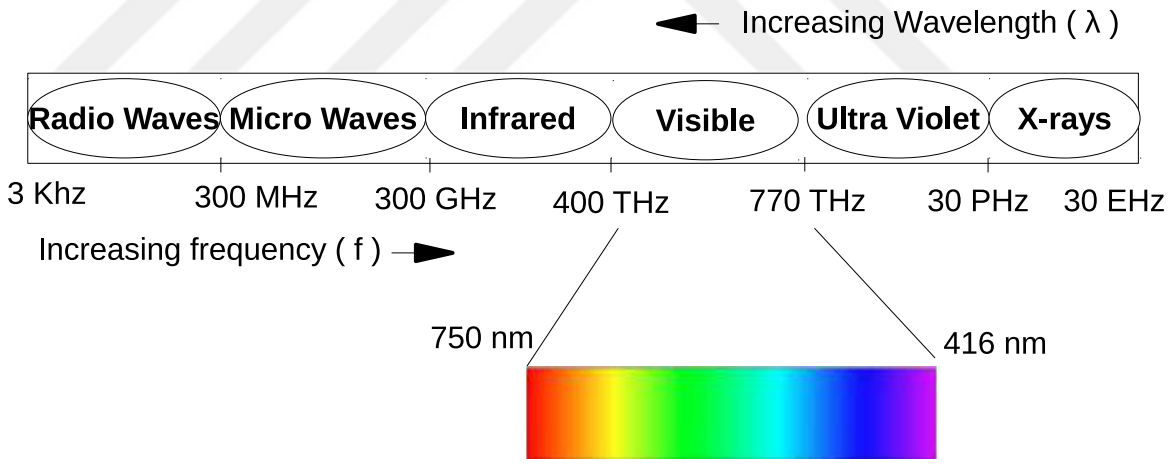

Figure 6: Frequency spectrum of communication signals and visible light colour distributions.

VLC employs frequency spectrum which is more than ten thousands times larger than RF spectrum as shown in Fig. 6. Therefore, the lack of bandwidth issue is resolved in VLC which provides secure data communication since the existing radio wave signals are able to pass through opaque materials while visible lights can not.

Other important property of visible light is the utilization of both environment illumination and communication. Therefore VLC system does not require any extra power. According to above advantages, VLC is one of the most popular candidates of future 5G wireless communication systems.

3.2 VLC System Architecture

In 2011, physical (PHY) and MAC layers are defined in IEEE 802.15.7 standard which was documented for short range visible light optical communication. A VLC architecture includes PHY, MAC and application layers as shown in Fig. 7. The

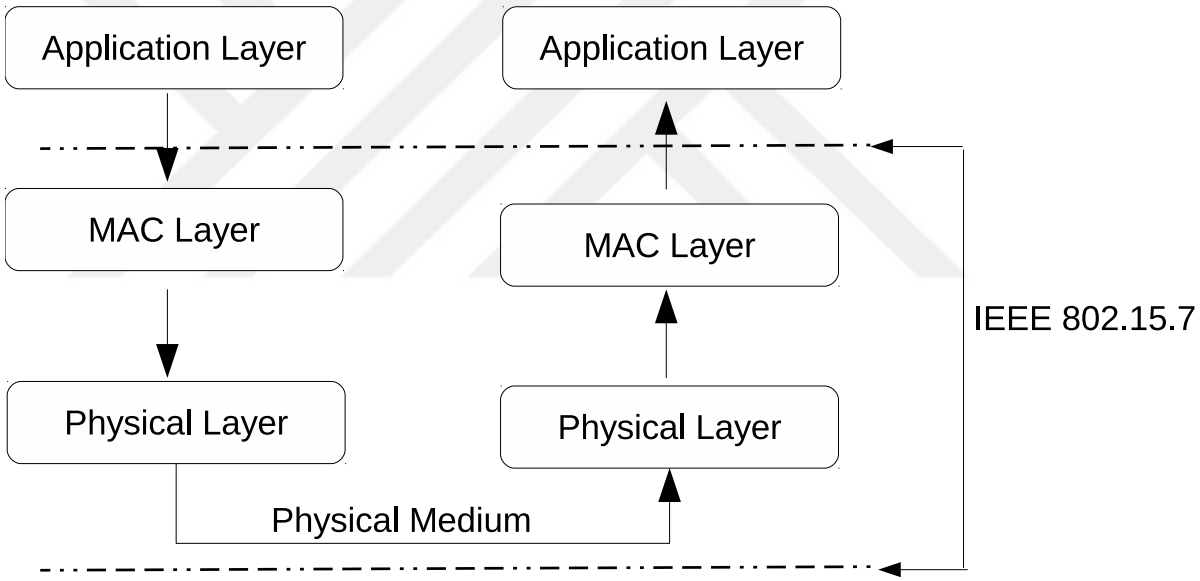

Figure 7: VLC architecture with layers including physical, MAC and application layers.

physical properties of the device and the relation between device and medium are comprised by the physical layer. The typical physical layer block diagram is shown in Fig. 8. The input data bits are modulated (such as ON and OFF keying, PPM and PWM etc.) after channel encoder block. Then, modulated bit stream is transmitted through optical channel by using LEDs as transmitter and photo diodes as receiver.

Instead of LED light bulbs and photo diodes, display based units and cameras can

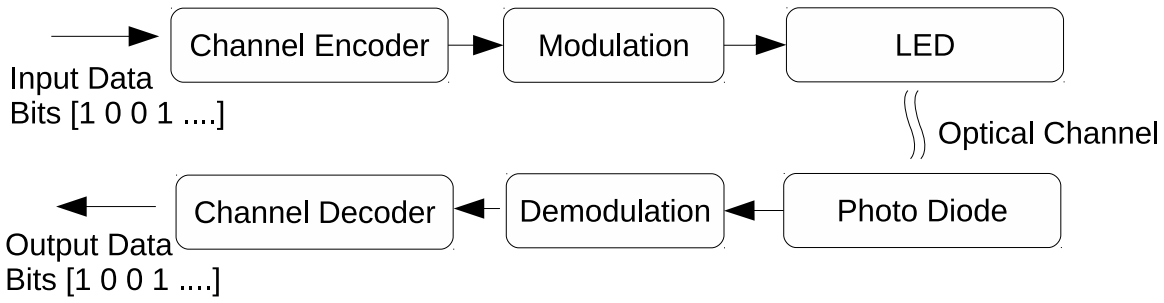

Figure 8: The block diagram of a typical physical layer [26].

be used as transmitter and receiver respectively. It creates a multiple input multiple output (MIMO) channel model as shown in Fig. 9.

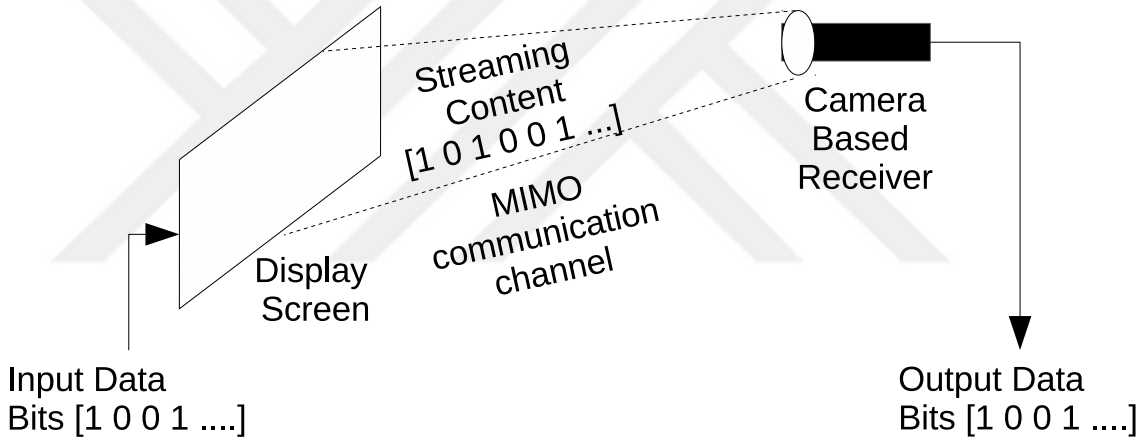

Figure 9: VLC MIMO channel model with display based transmitter and receiver based camera.

3.3 VLC Transmitter Types

In visible light communication any electronic device that can emit visible light can be a transmitter. In this section we mention about LEDs and display screens for using as a transmitter device in a VLC system.

3.3.1 VLC LED Transmitter

A light emitting diode (LED) is a type of diode that can emits light when it is triggered with a suitable current. The utilization of LED lights is increasing each day

Table 2: Comparison of lighting systems [39].

comparison	LED	incandescent light bulb	compact fluorescent(CFL)
Average Life Span(hours)	50000	1200	8000
Watts of electricity consumption(watts) (for 800 lumen output)	6-8	60	13-15
Annual Operating Cost($)	32.85	328.59	100
Switching time	fast	fast	slow

because the LED provides high performance (high luminosity with low current), low cost, fast response time (easy to switch on or off), and long life time compared to incandescent light bulb or CFLs. As shown in Table 2, LED is the first option for a VLC transmitter architecture.

3.3.2 VLC Display based Transmitters

Display screens are very popular for being widely used in laptops, TVs and mobile phones. Instead of using a single LED, a display screen can be used as a transmitter in a wireless optical communication. The pixel array of a display screen and the image sensor array of a camera may create multiple input multiple output (MIMO) elements of communication architecture to increase capacity. The capacity analyse of a structure including led emitting array (LEA) transmitter and camera receiver was given in [33]. The similar performance evaluation can be completed by considering display screen pixels as the LEA and taking into account the differences between them.

3.4 VLC Receiver Types

In visible light communication any electronic device that can detect visible light can be a receiver. In this section we mention about photo detectors and cameras for using as a receiver device in a VLC system.

3.4.1 VLC Photodetector based Receivers

Similarly to the rods in the eye retina, the photdetector is a light sensor that converts the light into electrical current. The light photons strike the material inside the photodetector and generate free electron which cause the electrical current. One of the important performance parameter of a photodetector is the speed. Modern photodetector can achieve up to tens of Gbit/s data rates. Photodetectors can be used in indoor wireless communication, as it can be used in outdoor long range applications. Tens of Kbit/s data rates are achieved in [41] while a few Gbit/s downlink speed is achieved in [40].

3.4.2 VLC Camera based Receivers

A camera is a practical device for a VLC since being existed in every modern smartphones. Main component of a camera is the imaging sensor including the array of photodetector that measures the light intensity for creating the captured image. Developed commercial image sensors can capture up to 60 frames per second (fps) with the 8K resolution (8192×4320 pixels) [42]. The maximum achieved speed with the VLC system with a camera receiver is dozens of MBit/s [8]. The sampling rate of a camera is lower than a photodetector since it consists of many photodetectors to form an image. On the other hand, VLC system with a camera receiver is a newer idea that has more space to be improved. Beside that, spatial dimension provided by MIMO channel model should be taken into account.

CHAPTER IV

DEVICE TO DEVICE (D2D) COMMUNICATION

4.1 Introduction

People spend their times more then they think with electronic devices since everything from cars and public places to the offices and houses are adorned with electronics. Therefore, almost every modern electronic devices include an input/output module that supports one or more communication type. In this chapter, D2D wireless communication types are introduced.

4.2 Applications

Communication techniques providing the data transmission between electronic devices change according to cost, size or usage area of the device. Various wireless device to device (D2D)communication systems have emerged in recent years such as DLNA, Bluetooth, near field communication (NFC) and barcode.

4.2.1 DLNA based Applications and Systems

Digital living network alliance (DLNA) is an organization consisting the participation of many consumer electronic companies to develop interoperability standard for sharing digital media between electronic devices within the local area netwrok (LAN). In 2016, the alliance released DLNA 4.0, supporting Ultra HD TV content streaming and extended multimedia format types [45]. However the development of wireless data communication architectures and the extension to the WiFi peer to peer (P2P) connection from LAN, decreased the popularity of DLNA which was dissolved in 2017 [43, 44, 46]. It is still one of the fastest interconnection type transferring massive information and it can achieve the data rates of IEEE 802.11 wireless communication

protocol.

4.2.2 BlueTooth Applications and Systems

Bluetooth is a wireless communication technique which provides data transmission among the electronic devices in 2.4 Ghz industrial, scientific, medical (ISM) band based on the standardization of IEEE 802.15.1 wireless personal area network (WPAN). It is intended to provide wireless short range, low cost, low power communication. Bluetooth is very popular in automotive applications for audio and remote control communication.

4.2.3 Barcode Applications and Systems

Barcode allows user to transfer data via printed symbols through visible light. Barcode systems have gained lots of implementation areas with the ubiquitous presence of smart phones. While primitive one dimensional barcode systems that have limited data capacity are used in shopping malls for inventory organization, matrix and QR codes have developed to increase the capacity for transferring relatively bigger data such as URL, payment information, advertising and device identification [47]. In [48,49], designed systems provide a temporal color barcode streaming between two screen achieving hundreds of Kbit/s throughput. While barcode applications provide more security due to nature of visible light it does not require handshaking procedure as in DLNA and Bluetooth applications.

4.2.4 Near Field Communication (NFC)

NFC is a short range communication (shorter than 4 cm) that enables robust, low speed, low power communication between two NFC compatible electronic devices for the purposes of contactless payment, multi-media file sharing etc. Although data communication with a throughput of hundreds of Kbit/s by bringing the devices close to each other seems practical, NFC still includes serious security issues [50, 51].

CHAPTER V

FOVLC: FOVEATION BASED DISPLAY TRANSMITTERS FOR VISIBLE LIGHT COMMUNICATION

5.1 Previous Works

Widespread availability of displays in TVs, computer screens and mobile phones as transmitters and cameras in mobile phones and low cost commercial or mobile phone cameras as receivers resulted in significant number of modulation methods and experimental studies in recent years [5–13, 20]. The visual data embedding should not distract the eye comfort of the user to preserve the functions of data communication and displaying images simultaneously. Thus researches have focused on 3 main challenges of the subject which are unobtrusive data hiding, communication channel capacity, transmission accuracy.

Existing systems generally use color or luminance properties of the video in spatial domain, temporal domain or frequency domain. As introduced in *Implicit Code* [5], the system is no real time, average throughput is over 45 Kbit/s with decoding accuracy of more than 90%. Colour translucency is manipulated spatially rather than color. The translucency basically controls the color intensity of the original video. Visually, the video can be dimmed or brightened by adjusting this parameter. To decrease the flicker effect video is displayed at high frame rate (120 Hz) and recorded at 240 Hz. So *Implicit Code* is a spatio temporal system. Generally the methods introduced in *Hi-Light* [7] and *InFrame* [6] are combined. In [6] and [7] the system is no real time, less than 10 Kbit/s throughput, higher frame rate display is needed to operate. *Hi-Light* encodes the data by adjusting the translucency (opacity) of

sub-pixels of panel cell. It means there is no any digital operation on image. Instead system benefits from device hardware. In [6], data is modulated by manipulating the brightness level of pixel blocks of sequential frames. So the original message is retrieved by analysing the difference of sequential frames in temporal domain. *InFrame* was improved by having spatio-temporal structure in 2015 [20]. And the average capacity is between 150-240 Kbit/s. Real time implementation of *Hi-Light* was experienced as well [9] and it achieves up to 1.1 Kbit/s throughput with accuracy of more than a ratio between %84-%91. *IVC:Imperceptible video communication* [8] theoretically can achieve up to 26 Mbit/s, but there is no detailed simulation and accuracy result. In *Photographic Steganography* [10] a differential metamer set is defined to modulate message optimally in the form of color shift. The differential metamer set simply includes original color coordinates, optimum color shift direction and color shift amount in Lab color space. Therefore the message-embedded image is created by a color shift with a direction depending on the coordinates of the specified color in Lab color space. But the best accuracy result of the system is still 90% although the embedded message is visible. There are other methods that uses high speed LED array dimming to provide communications [21, 25].

All the above related studies try to hide message information to the entire image uniformly. However, human visual system (HVS) has a special foveation property where the distraction outside the eye focus point gets smaller in a way that data hiding capacity can be improved significantly in an adaptive manner [4]. In this article, foveation property is utilized to design and implement a novel modulation method denoted by "FoVLC" by adaptively increasing color shifts in areas out of focus of the viewer to decrease bit error rate (BER) of data transmission. The method uniformly performing data hiding throughout the screen by using color shifts in pixels is denoted by *conventional method*. Proposed proof of concept design achieves to decrease BER compared with the conventional method for simple experimental set-up with TV

Table 3: Modelling constants for cell density in HVS [19].

Meridian	k	a_k	$\Theta_{2,k}$	σ_k	$d_c(0)$	Θ_m
Temporal	1	0.9851	1.058	22.14	14804.6	41.3
Superior	2	0.9935	1.035	16.35		
Nasal	3	0.9729	1.084	7.633		
Inferior	4	0.996	0.9932	12.13		

based transmitter and commercial camera based receiver architecture.

5.2 System Model

FoVLC system includes a display transmitter with display screen pixel size $M \times N$ while it is assumed that the eye focus of the viewer is tracked with a camera based receiver in coordination with the transmitter as shown in Fig. 10. Focusing point is modelled with viewing angle (ϕ), eccentricity (Θ) and the distance of the eye denoted by u to the focal point with the center $F \equiv (f_v, f_h)$. Modulation is performed by modulating color values of pixel blocks denoted by grid message block (GMB). Each GMB has pixel size of $GMB_v \times GMB_h$ while the total number of blocks is given by $df_v \times df_h$ where $GMB_v \equiv M \,/\, df_v$ and $GMB_h = N \,/\, df_h$. Color values in each GMB is adaptively shifted in CIE xyY color space. Next, HVS is modeled in terms of the density of photo receptors with respect to Θ. HVS is very sensitive to the details, i.e., luminance and color variances around the point of fixation as shown in Fig. 10 where eye gaze is focused on. Sensitivity falls rapidly with increasing eccentricity [16].

5.2.1 The Mathematical Model of HVS Spatial Resolution

Perception of details changes according to eccentricity (Θ) as a parameter describing HVS spatial resolution. The most effective factor determining perception performance of color variations is the density of midget retinal ganglion cell receptive field [19], as mentioned in Section 2.2.2 and it is denoted by d_m. Since the retina is not symmetric around the retinal center, d_m is different along four principal meridians which are temporal, superior, nasal, inferior as shown in Fig. 5. d_m is the function of Θ and

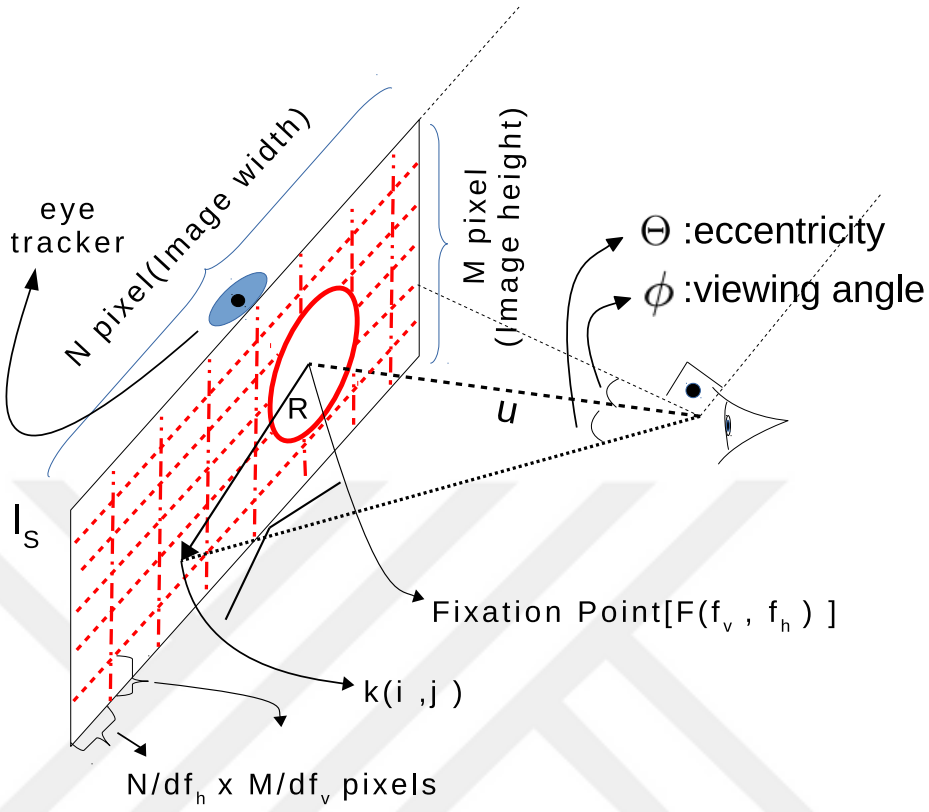

Figure 10: FoVLC system model where ϕ is the viewing angle, i.e., the angle between the trajectory of eye and normal line of the screen, Θ (eccentricity) is the angular distance between eye focus point (fixation point) denoted by $F = (f_v, f_h)$ and grid message block (GMB), R is the Euclidean distance of the center of GMB to F, the screen size is $M \times N$ pixels, u is the distance between eye and F, the number of GMBs is $df_v \times df_h$ and $0 < f_v < M$ and $0 < f_h < N$.

meridian index (k) and defined as follows:

$$d_m(\Theta, k) = 2\, d_c(0) \left(1 + \frac{\Theta}{\Theta_m}\right)^{-1} \times \left[a_k \left(1 + \frac{\Theta}{\Theta_{2,k}}\right)^{-2} + (1 - a_k)\, exp\left\{ - \frac{\Theta}{\sigma_k}\right\}\right] \quad (1)$$

where $d_c(0)$ is the cone density (cone/deg^2) at foveal zone, $\Theta_m = 41.3°$ is the scale factor for decline in midget fraction with Θ, $\Theta_{2,k}$ is eccentricity at which the spacing is doubled (deg), a_k is the weighting of the first term, σ_k is the scale factor of the exponential as shown in Table 3. Assume that d_m is the same for all retinal indices of temporal, superior, nasal and inferior and takes the coefficients of superior index.

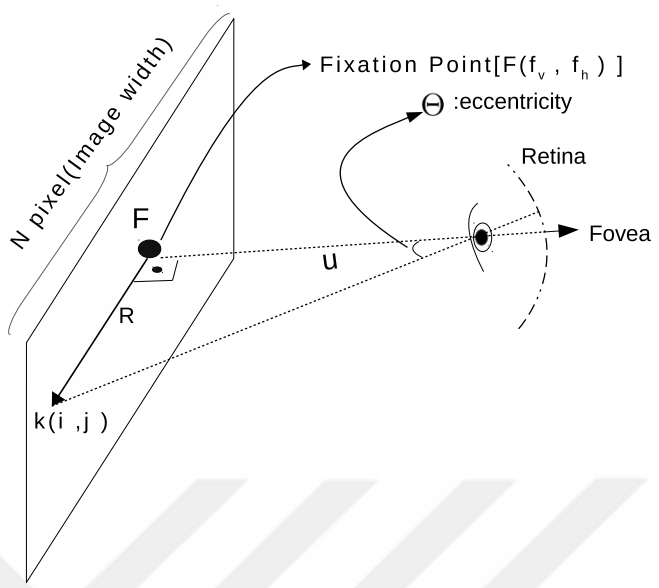

Figure 11: The geometrical relationship between eccentricity and spatial distance [37].

Then, d_m is simplified as follows:

$$d_m(\Theta) = 2\, d_c(0) \left(\frac{41.3}{41.3+\Theta}\right) \times \left[0.9935 \left(1+\frac{\Theta}{1.035}\right)^{-2} + 0.0065\, exp\left\{-\frac{\Theta}{16.35}\right\}\right] \tag{2}$$

Θ of each pixel changes according to the position of pixel where human eye gaze is focused on, i.e., the position F of eye focus. There are four visual fields on display screen as shown in Fig. 5. Euclidean distance of any pixel with the index (i, j) to F is $R(i,j) = \sqrt{(i-f_v)^2 + (j-f_v)^2}$ and utilized to find relation between Θ and distance R in spatial domain shown in Fig. 11. Then, Θ is approximated as follows by neglecting viewing angle around the normal line of display, i.e., $\phi = 0$:

$$\Theta(u, R) = tan^{-1}(R \,/\, N\, u) \tag{3}$$

where u is the normalized distance of eye from the display screen represented as multiple of N in pixel units.

In Fig. 12(a), d_m and Θ are shown for varying R. Consider a TV screen with resolution HD (720×1280) and size 28 inch while the viewer eye stands 78 cm away

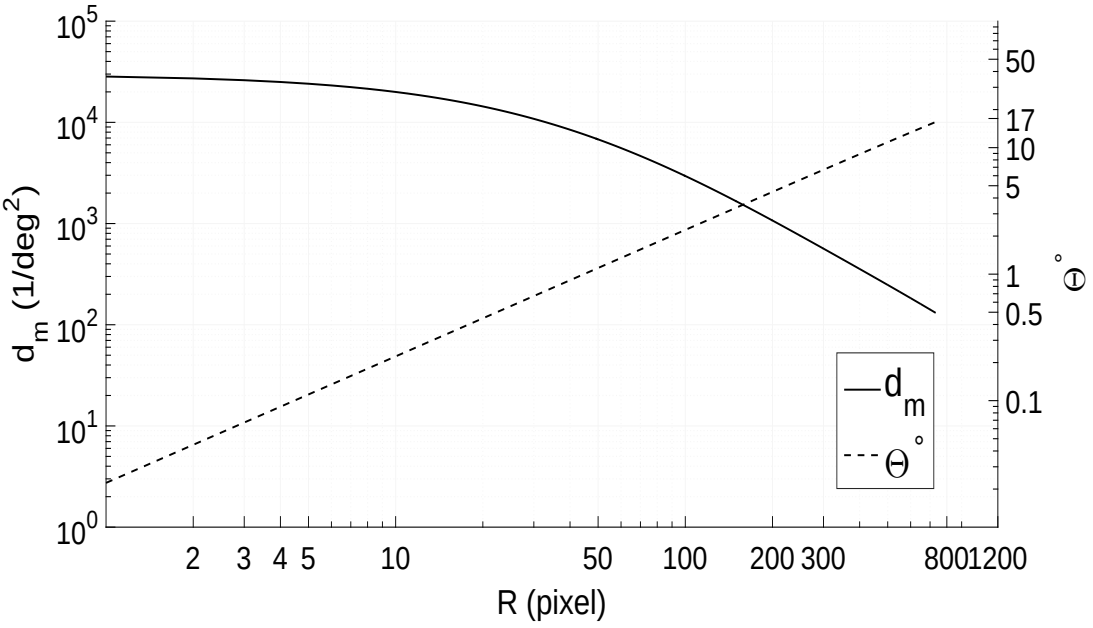

(a)

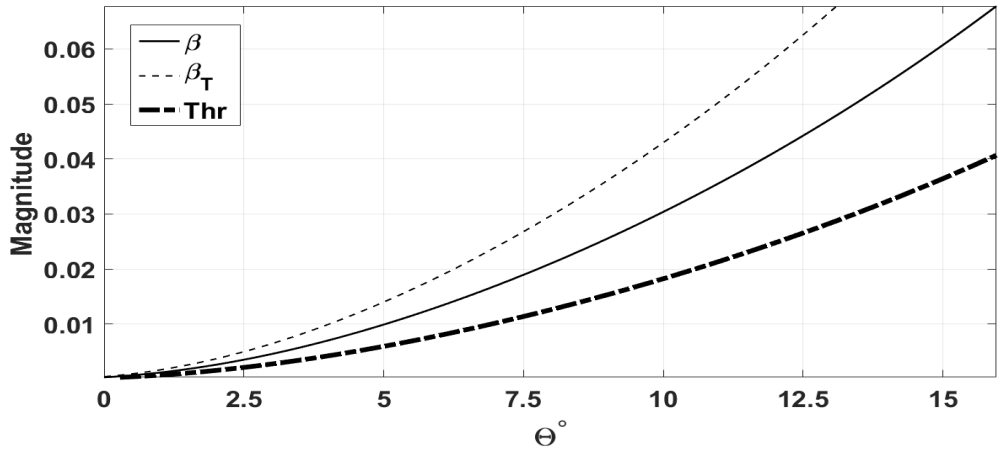

(b)

Figure 12: (a) d_m and Θ for varying R where $M \times N = 720 \times 1280$, F is assumed at the middle of the screen, i.e., $(fv, fh) = (360, 640)$, $u = 2 \times N$, and (b) the magnitudes of β (the amount of chromaticity shift in xyY domain modelled according to Θ), β_T and Thr defined as $\approx 0.6\,\beta$ for varying Θ.

from the center of display and image width on the display is $N = 38.8$ cm. (i.e. $u \approx 2$) If the eye is focused to the center, then the ability to perceive color variations on the edge of image (with $\Theta \approx 15°$-$17°$) decreases ≈ 170 times with respect to the one in the center. It is inversely proportional to d_m. Therefore, chromaticity shift

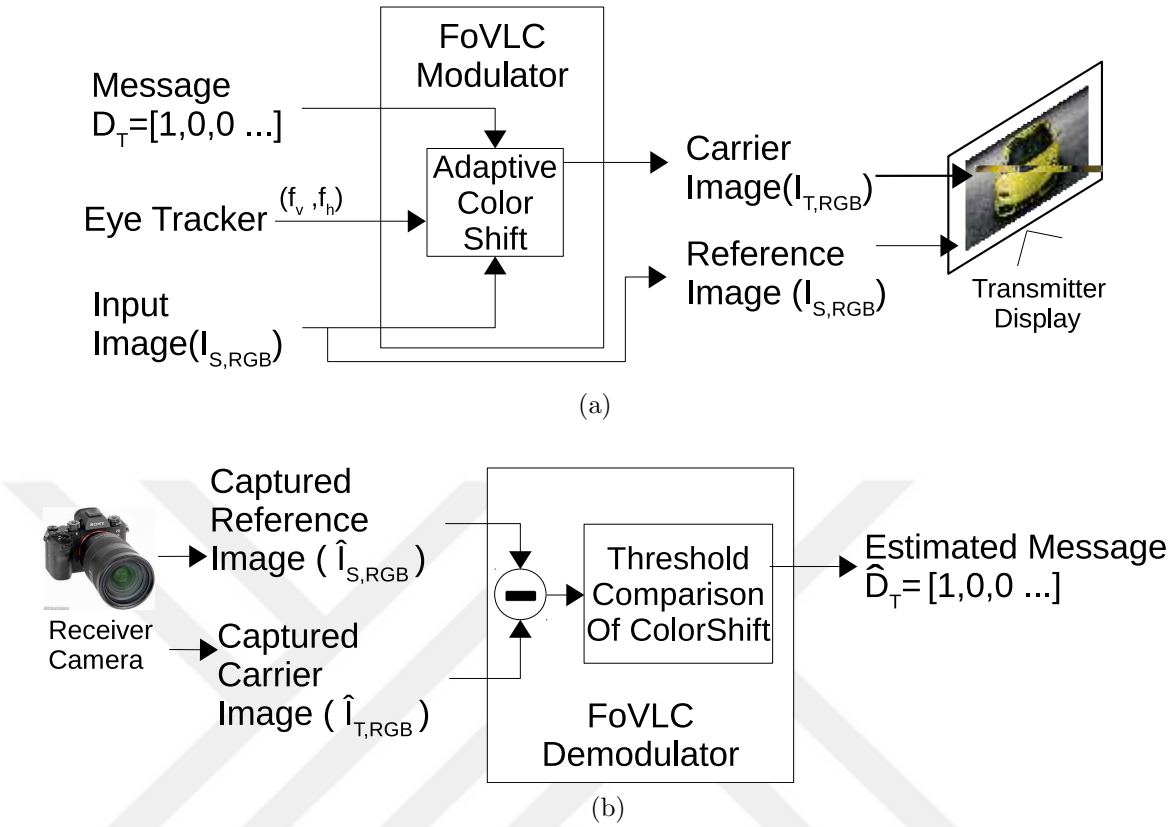

Figure 13: System block diagram for FoVLC system where (a) modulation and (b) demodulation block diagrams are given. Transmitter side modulates message bits represented with the vector $\mathbf{D}_T$ on input reference image $\mathbf{I}_{S,RGB}$ based on focus point F and generates carrier image $\mathbf{I}_{T,RGB}$ while the receiver captures sequential screen shot of both $\mathbf{I}_{S,RGB}$ and $\mathbf{I}_{T,RGB}$. The difference of $\mathbf{I}_{S,RGB}$ and $\mathbf{I}_{T,RGB}$ is compared with a threshold level denoted by Thr to estimate original message vector.

factor (β) in FoVLC system is increased by starting at F and combining (2) and (3) as follows:

$$\beta(\Theta) = \frac{d_m(\Theta = 0) \times \beta(\Theta = 0)}{d_m(\Theta)} \tag{4}$$

Minimum value of $\beta(\Theta = 0)$ is set to 0.0003 so the value of β around 2° of F is kept at 0.0025 accepted as just noticeable difference (JND) being arithmetic mean of major and minor radial lengths of 25 different Mac Addam ellipses [22] which are shown in Fig. 14. Magnitude of $\beta(\Theta)$ for varying Θ is shown in Fig. 12(b).

FoVLC performs data hiding method by shifting color in the modulated areas similar to photographic steganography in [10] while limiting the modulated area to

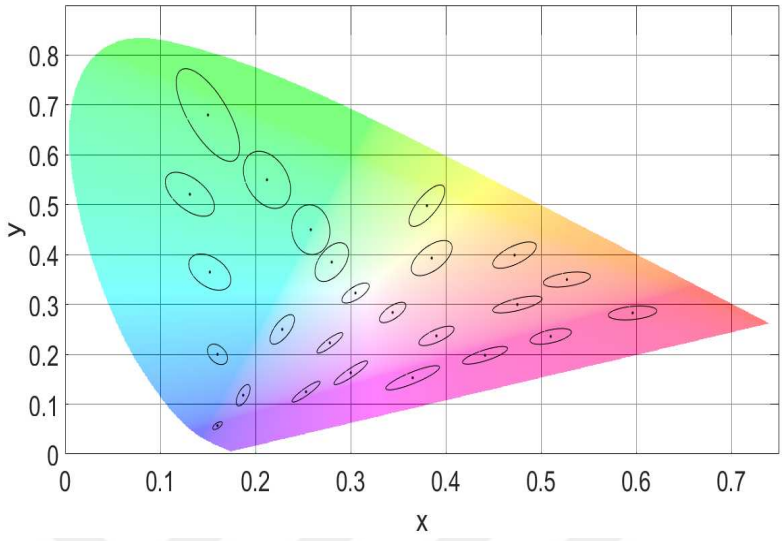

Figure 14: Twenty five different Macaddam ellipses sketched over CIE-1931 xy chromaticity diagram. The sizes of ellipses are enlarged by ten for the purpose of demonstration. It is adapted from the table in [22].

outside of focal region in an adaptive manner. Next, the details of FoVLC modulation and demodulation mechanisms are discussed.

5.3 Modulation and Demodulation Algorithms

System block diagram for FoVLC modulation and demodulation set-ups are shown in Figs. 13(a) and (b), respectively. Main system components are described in the following list while the algorithms are given for both FoVLC and conventional methods in Algorithms 1 and 2, respectively:

5.3.1 Input Image Generation

Initially, 8 bit RGB image denoted by $\mathbf{I}_S$ is read with a picture size of $M \times N$ pixels. The value of a pixel is given in RGB format as follows:

$$\mathbf{I}_{S,RGB}(i,j) = \Big(I_S^R(i,j), I_S^G(i,j), I_S^B(i,j)\Big) \tag{5}$$

where $i \in [1,\, M]$ and $j \in [1,\, N]$.

5.3.2 Color Space Conversion (CSC)

$\mathbf{I}_S$ is converted into CIE xyY color space to take action on luminance and chromaticity components of image separately. The image pixel value in xyY format is represented as follows:

$$\mathbf{I}_{S,xyY}(i,j) = \Big(I_S^x(i,j), I_S^y(i,j), I_S^Y(i,j)\Big) \tag{6}$$

5.3.3 Modulator

xyY image is divided into GMBs which are modulated for each message bit. The smaller block size means more bits per frame transmission but higher BER in the receiver. GMB centers $\mathbf{c}^{m,n}$ are indexed with $(m,\ n)$ as follows:

$$\mathbf{c}^{m,n} = \Big((m+0.5)\,GMB_v,\ (n+0.5)\,GMB_h\Big) \tag{7}$$

where $0 \leq m \leq df_v - 1$ and $0 \leq n \leq df_h - 1$. R, Θ and β are calculated based on $\mathbf{c}^{m,n}$ of each GMB and F as shown in eq. (3) and (4). If Θ is smaller than 2.2°, then there is no encoding since 2° is in focal area and low amount of color shift is allowed. The focal region is set to 2.2° calculated according to $\mathbf{c}^{m,n}$. Modulated color values of the pixels in GMB with the indices (m,n) are given as follows:

$$\mathbf{I}_{T,xyY}^{m,n} = \begin{cases} \mathbf{I}_S^{x,m,n} + \beta(\Theta)\,d_T, \\ \mathbf{I}_S^{y,m,n} + \beta(\Theta)\,d_T, \\ \mathbf{I}_S^{Y,m,n} \end{cases} \tag{8}$$

where $\mathbf{I}_{T,xyY}^{m,n}$, $\mathbf{I}_S^{x,m,n}$, $\mathbf{I}_S^{y,m,n}$ and $\mathbf{I}_S^{Y,m,n}$ denote image matrices corresponding to the GMB with the indices (m,n) and $\beta(\Theta)$ defines the amount of colour shift as shown in Fig. 12(b). $\mathbf{I}_T$ denotes the modulated carrier image. If the incoming message bit (d_T) is zero then there is no color shift. In conventional method, β does not depend on Θ and fixed as 0.02 which is high enough to be visible on image. At the end of modulation process, carrier image $\mathbf{I}_{T,xyY}$ is created and converted back to RGB.

Algorithm 1 Modulation Algorithm

Input Image: $\mathbf{I}_{S,RGB}$
CSC: $\mathbf{I}_{S,xyY} \leftarrow \mathbf{I}_{S,RGB}$
Image to GMB conversion: $\mathbf{I}_S^{m,n} \leftarrow \mathbf{I}_{S,xyY}$
for `n=1,n++,n` $\leq df_h$ **do**
  for `m=1,m++,m` $\leq df_v$ **do**
    if FoVLC method **then**
      Input the output of Eyetracker: F
      Calculate R and Θ
      if ($\Theta \geq 2.2^\circ$) **then**
        Calculate $d_m(\Theta), \beta(\Theta)$
      else $\beta = 0$ ▷ focal area, no data encoding
      end if
      Apply equation (8) ▷ $\mathbf{I}_{T,xyY}^{m,n}$
    end if
    if Conventional method **then**
      $\beta = 0.02$
      Apply equation (8) ▷ $\mathbf{I}_{T,xyY}^{m,n}$
    end if
  end for
end for
GMB to image conversion : $\mathbf{I}_{T,xyY}(i,j) \leftarrow \mathbf{I}_{T,xyY}^{m,n}$
ICSC : $\mathbf{I}_{T,RGB} \leftarrow \mathbf{I}_{T,xyY}$ ▷ Carrier Image

5.3.4 Display & Camera

$\mathbf{I}_S$ and $\mathbf{I}_T$ are both effected by viewing angle of the camera, camera initial settings (ISO sensitivity, shutter speed, aperture, white balance), perspective distortions and environmental conditions. Since these factors are almost the same during sequential screen shot, $\mathbf{I}_S$ and $\mathbf{I}_T$ frames are assumed to have similar channel effects.

5.3.5 Scaler & Perspective Correction

Captured RGB reference and carrier images denoted by $\widehat{\mathbf{I}}_S$ and $\widehat{\mathbf{I}}_T$, respectively, are geometrically edited and rescaled.

5.3.6 Demodulator

For message recovery, the difference matrix, $\boldsymbol{\Delta}_I = \sqrt{(\widehat{\mathbf{I}}_{T,x} - \widehat{\mathbf{I}}_{S,x})^2 + (\hat{\mathbf{I}}_{T,y} - \widehat{\mathbf{I}}_{S,y})^2}$ in xyY color space is calculated and divided into $df_v \times df_h$ size matrices where $\boldsymbol{\Delta}_I^{m,n}$

Algorithm 2 Demodulation Algorithm

Input captured images: $\hat{\mathbf{I}}_T, \hat{\mathbf{I}}_S$
Scaler & Perspective correction
CSC : $\hat{\mathbf{I}}_{T,xyY}, \hat{\mathbf{I}}_{S,xyY} \leftarrow \hat{\mathbf{I}}_{T,RGB}, \hat{\mathbf{I}}_{S,RGB}$
$\boldsymbol{\Delta}_I \leftarrow ||\hat{\mathbf{I}}_{T,xy} - \hat{\mathbf{I}}_{S,xy}||$
Image to GMB conversion: $\boldsymbol{\Delta}_I^{m,n} \leftarrow \boldsymbol{\Delta}_{I,xyY}$
Input the output of eye tracker: position F
for `n=1,n++,n` $\leq df_h$ **do**
  for `m=1,m++,m` $\leq df_v$ **do**
    if FoVLC method **then**
      Calculate R, Θ, $d_m(\Theta)$ and $\beta(\Theta)$
      if ($\Theta \geq 2.2^\circ$) **then**
        if $\beta_T(\Theta) \geq Thr(\Theta)$ **then** $\hat{d}_T \leftarrow 1$
        else $\hat{d}_T \leftarrow 0$
        end if
      else ▷ Focal region, no data extracted
      end if
    end if
    if Conventional method **then** $\beta = 0.02$
      if $\beta_T \geq Thr$ **then** $\hat{d}_T \leftarrow 1$
      else $\hat{d}_T \leftarrow 0$
      end if
    end if
    Combine estimations: $\hat{\mathbf{D}}_T \leftarrow \hat{d}_T$
  end for
end for

Figure 15: The extensive image set used in experimental studies where images have increasing index numbers between one and twelve starting from top left to the bottom right.

denotes the matrix corresponding to the GMB with the indices (m, n). Borderlines of each $\boldsymbol{\Delta}_I^{m,n}$ might have unstable pixel color variations, thus each GMB is multiplied

by a 2D Hanning window ($\mathbf{H}$) of the same size that has an average value of unity. Then, average magnitude of each GMB is calculated as follows:

$$\beta_T(\Theta) \equiv \overline{\mathbf{\Delta}_I^{m,n} \bullet \mathbf{H}} \tag{9}$$

where $\beta_T(\Theta)$ denotes the average magnitude of the dot-product of ($\mathbf{H}$) and $\mathbf{\Delta}_I^{m,n}$. In conventional method, β_T does not depend on Θ and compared with the threshold parameter (Thr) as follows:

$$\hat{d}_T = \begin{cases} 1, \ \textit{if } \beta_T \geq Thr \\ 0, \ \textit{if } \beta_T \leq Thr \end{cases} \tag{10}$$

Thr is tuned to some multiple $k\,\beta(\Theta)$ for $k \in [0,\, 1]$, i.e., $k = 0.6$, obtained empirically to get the minimum BER. In ideal case (no channel or camera distortion), $\beta_T(\Theta)$ is expected to be $\sqrt{2} \times \beta(\Theta)$. Magnitudes of Thr and $\beta_T(\Theta)$ are shown in Fig. 12(b). R, Θ, $d_m(\Theta)$, $\beta(\Theta)$ are calculated based on $\mathbf{c}^{m,n}$ and F. FoVLC demodulation includes the following steps:

1. If Θ of $\mathbf{c}^{m,n}$ (with respect to F) is smaller than 2.2°, then GMB is too close to F and there is not any encoded message. Focal area is indicated with red in Fig. 16(h).

2. If $\Theta > 2.2°$, then it means that GMB has modulation data. Then, $\beta_T(\Theta)$ is compared with Thr as follows:

$$\hat{d}_T = \begin{cases} 1, \ \textit{if } \beta_T(\Theta) > Thr \\ 0, \ \textit{if } \beta_T(\Theta) < Thr \end{cases} \tag{11}$$

Finally, $\hat{d}_T$ bits are combined in $\hat{\mathbf{D}}_T$.

5.4 Experimental Tests

Theoretical and experimental modeling of the system is based on captured still images however proposed FoVLC modulation allows data communication over video frames

Table 4: System parameter default values

Parameter	Value
$M \times N$	720×1280 (pixels)
$df_v \times df_h$	12×16, 20×20, 40×40, 60×80
β	0.02 (conventional method), function of Θ (FoVLC)
Thr	$0.6 \times \beta$
Focal area angle	2.2°
$F = (f_v, f_h)$	(360, 640)
u	$\{1, 1.1, 1.2, \ldots, 2.4, 2.5\}$
ϕ	0°
Θ	function of u, N and R

by predicting or detecting the viewer's region of interest with the methods such as mentioned in [23, 24], and then analyzing and optimizing color properties and modulation for each video frame. The data rate is proportional to the number of individual frames similar to the conventional display based VLC modulation methods [33].

For the experimental study, foveated and conventional methods are implemented on MATLAB for the parameters given in Table 4 based on the standard color temperature (9300 K, x=0.285, y=0.293) of a 28 inch LCD TV display setting under an ambient light of regular office (301 lux measured by a JETI spectroradiometer). Focal area is specified around 2.2° of F so that transmitted bits per frame are decreased for FoVLC while eye comfort and accuracy are increased. Logitech webcam (C310) and a set of twelve 8-bit display images are used as shown in Fig. 15. Images are experimented repetitively for varying ($df_v \times df_h$) and viewer distance coefficient (u) specified as in Table 4. Checker board pattern is used as the message matrix and F is accepted as the middle of the screen. At the end of each iteration, $\mathbf{D}_T$ and $\hat{\mathbf{D}}_T$ are compared. The number of transmitted bits depends on $df_v \times df_h$ in conventional method while it also depends on viewer distance in FoVLC since increasing viewer distance results in larger focal area. It is observed that message data is visible on the road for conventional method while invisibility is provided in focal region for FoVLC

as shown in Figs. 16(a) and (b) showing $\mathbf{I}_{T,RGB}$ images. Figs. 16(c) and (d) show β magnitude of each GMB. $\beta(\Theta)$ on the white circle is 0.02 which is constant in conventional method. Figs. 16(e) and (f) show $\mathbf{\Delta}_I$ matrices while Figs. 16(g) and (h) show estimated messages.

In Fig 17(a), BER of six different images are shown while average BER of the set for varying u and $df_v \times df_h$ is shown in Fig. 17(b). If the viewer is positioned close to the screen, e.g., normalized $u \approx 1$ for a notebook, more color shift is allowed for outside of the focal region providing better data transmission performance. As the viewer distance is increased, HVS has wider vision resulting in a decrease in the allowed color shift as shown in Fig. 17(c). Highly textured images provide better hiding and higher BER while BER is lower for low frequency image regions. FoVLC gives better results for such textured images where BER for the image indexed with 6 is shown in Fig. 17(a) as 28% for FoVLC while 42% for conventional method. Moreover, pixel colors having relatively higher values (yellowish or greenish hue) are saturated with color shift due to limited color range of sRGB scale. In Figs. 16(g) and (h), it is shown that message cannot be decoded on yellowish green regions such as tree or grass in both methods.

In conventional method, messages are generally visible on the carrier image. FoVLC method provides better data invisibility to the user with experimental tests performed with people subjects. Carrier and reference image sets are shown on two identical display screens of 42 inch TV where people subjects are placed at the normalized position of $u = 2$. They are asked yes or no questions about the similarity of two images while changing eye focus in a random manner. As a result, 8 participants out of total 10 feel the difference only in two images among the set of twelve images while two participants does not feel any difference. This shows the success of FoVLC modulation mechanism.

5.5 Discussion

In this section, simplifying assumptions in our model are discussed.

5.5.1 Assumptions

We have made the following assumptions in our model to simplify mathematical modelling and experimental studies:

- Algorithms are performed on still images captured at a specific time while extension to the dynamic video frames is left as a future work.
- We have assumed the availability of an eye tracking software continuously monitoring the movements of eyes in order to set foveation point on the image. There are various tracking methods available in the literature [23, 24].
- Symmetric retinal ganglion cell distribution over four principal retinal meridians in order to simplify HVS mathematical modelling.

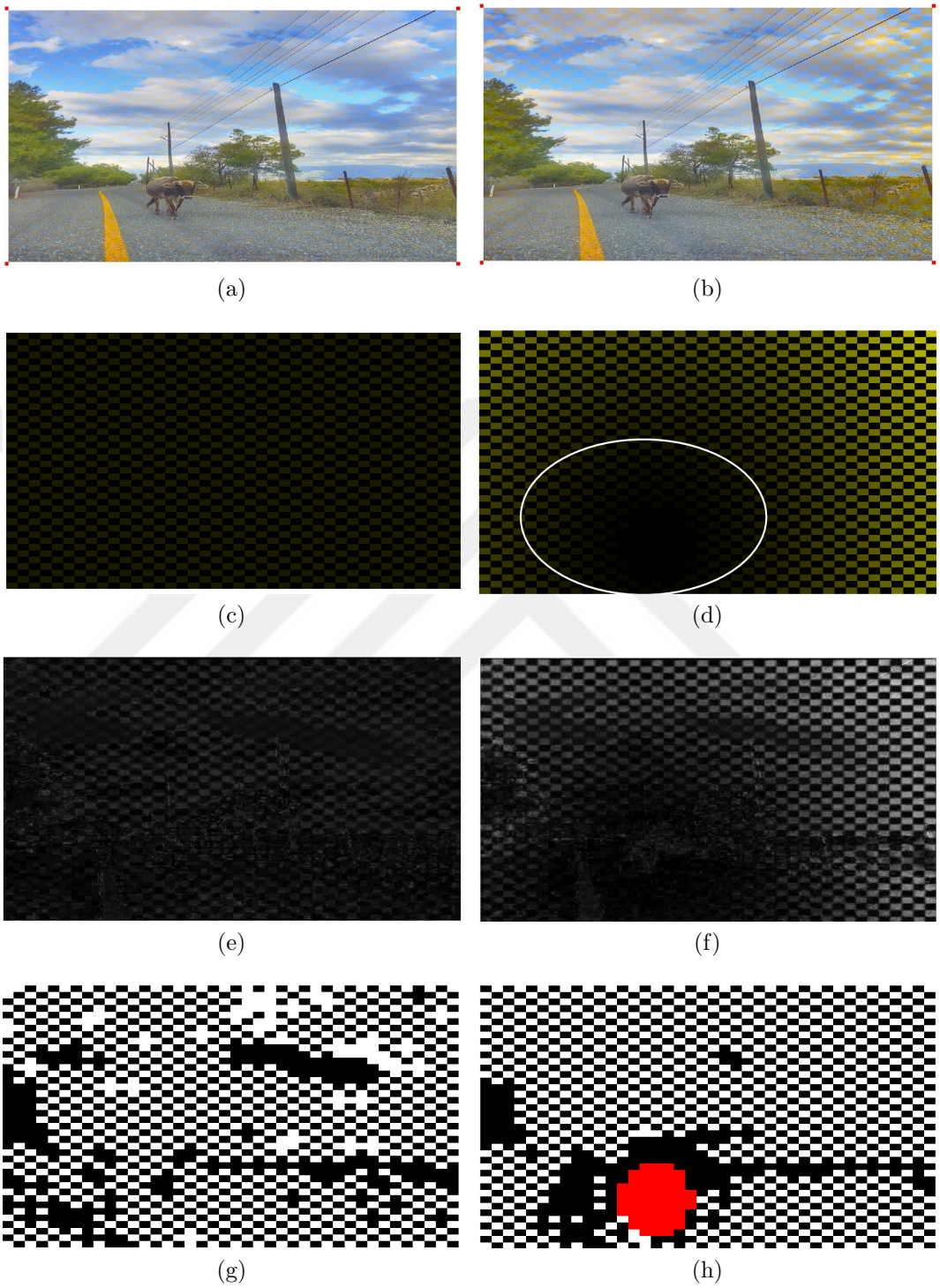

Figure 16: Right and left sides show conventional and FoVLC images, respectively, where (a) and (b) show message embedded images with square shaped red corners utilized in scaling and perspective corrections, (c) and (d) show color shift applied to each GMB, (e) and (f) show $\boldsymbol{\Delta}_I$, and (g) and (h) present estimated message blocks for each GMB where red area is not modulated in FoVLC. Interior of white circle in (b) indicates β lower than 0.02 which is constant for conventional method. F is assumed as $(f_v, f_h) = (583, 493)$. Each picture has 40×40 GMBs where the number of modulated bits are 1600 and 1541 for conventional and FoVLC respectively. (In (c), (d), (e) and (f) image magnitudes are expended by 5 for the purpose of demonstration)

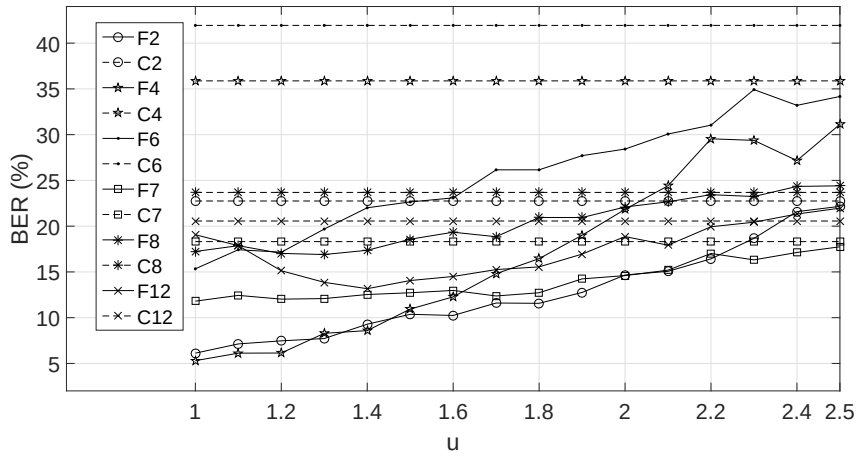

(a)

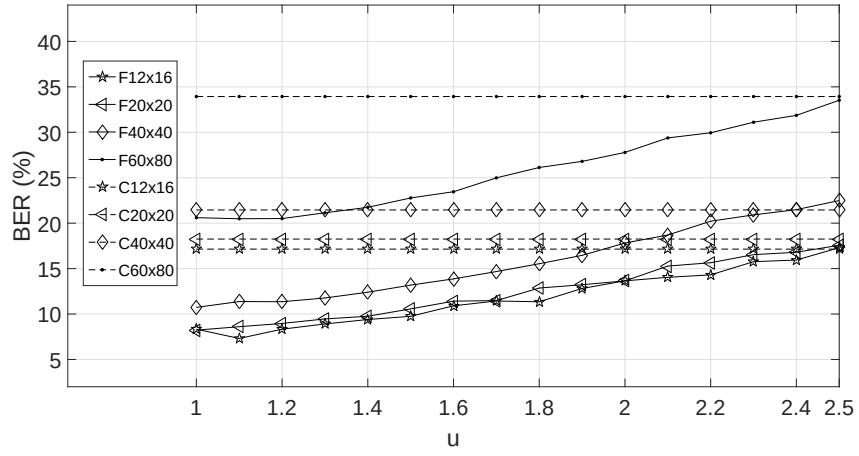

(b)

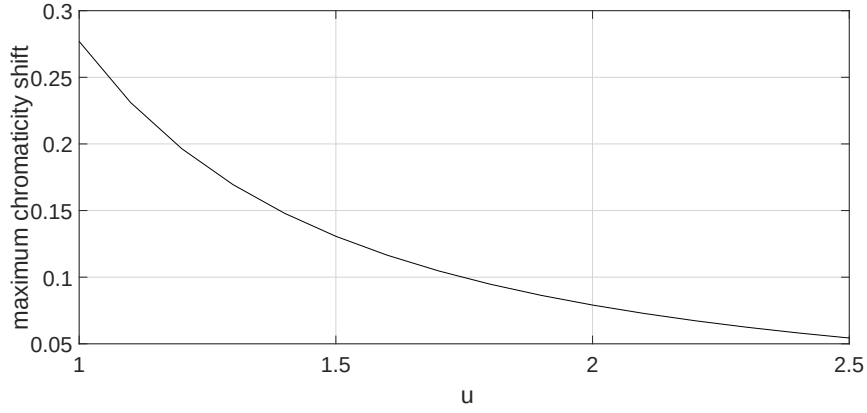

(c)

Figure 17: (a) BER for six different images for both conventional (denoted by C) and FoVLC (denoted by F) methods where $df_v \times df_h = 40 \times 40$ and the image indices are given after the methods, (b) average BER for varying u and $df_v \times df_h$ values of 12×16, 20×20, 40×40 and 60×80, and (c) maximum color shift (maximum β) on the corners of display screen for varying u. Note that, for $u = 2.5 \times N$, color shift is $\beta = 0.05$ at the edges of the screen while spatially uniform color shift is $\beta = 0.02$ for conventional method.

CHAPTER VI

CHALLENGES AND OPEN ISSUES

The following list includes open issues to optimize FoVLC system design and to realize performance improvements compared with the proposed simple set-up as a proof of concept:

- Theoretical modelling of performance with respect to the system parameters including GMB block sizes, distance, orientation, light intensity and interference while also considering the effects of source and channel coding.
- Optimization of block sizes and utilizing error correction for given system parameters.
- Modulation with a wider color gamut, i.e., DCI-P3, NTSC, Rec. 2020. In the proposed study, increasing x and y component of each GMB color and the limited color range of sRGB domain causes saturation on greenish and yellowish hues or peripheral area of image.
- Experimental study with bigger size and resolution display screens. In the proposed experiments, focal area cover most of the display screen causing a decrease in total transmitted bits with a long viewer distance and small sized display screen.
- Optimization of screen and camera optical properties. It is observed that using inverse transmitter display white point and receiver camera white balance settings improves the performance of the system in some circumstances requiring detailed experimental simulations to clearly define.

CHAPTER VII

CONCLUSION

In this thesis, theoretical design and experimental tests of a novel VLC modulation method denoted by FoVLC is performed. The proposed method adaptively modulates color shift based data hiding modulation amplitude in display transmitters based on the eye focus point of the viewer. Modulation and demodulation algorithms are presented and experimental tests are performed for simple system architecture with TV based display transmitter and camera based receiver architecture. FoVLC method is compared with the conventional method which uniformly modulates the color shifts throughout the screen showing that average BER drops approximately to half of the value for the set-up as a prof of concept while not distracting test participants. Future works and open issues to optimize system design are discussed.

Bibliography

[1] S. Rajagopal, R. D. Roberts and S. K. Lim, "IEEE 802.15.7 visible light communication: modulation schemes and dimming support", *IEEE Communications Magazine*, vol. 50, no. 3, pp. 72-82, 2012.

[2] B. Gulbahar and S. Sencan, "Wireless internet service providing for 5G with hybrid TV broadcast and visible light communications", *Proc. of The IEEE IFIP Wireless Days (WD)*, pp. 29-31, 2017.

[3] B. Gulbahar and S. Sencan, "Method for wireless internet service providing for 5G with hybrid TV broadcast and visible light communications", EP17175972.3, *EPO Patent Application*, June 2017.

[4] B. Gulbahar, O. Yildiz, "Foveation based unobtrusive and stenographic ultra-high rate visible light communication system and method", PCT/EP2016/081998, *EPO Patent Application*, January 2017.

[5] S. Shi, L. Chen, W. Hu, and M. Gruteser, "Reading between lines: high-rate, non-intrusive visual codes within regular videos via ImplicitCode", *In Proc. of the ACM 2015 International Joint Conference on Pervasive and Ubiquitous Computing*, pp. 157 168, 2015.

[6] A. Wang, C. Peng, O. Zhang, G. Shen, and B. Zeng, "Inframe: Multiexing full-frame visible communication channel for humans and devices", *In Proceedings of the 13th ACM Workshop on Hot Topics in Networks*, pp. 23-30, 2014.

[7] T. Li, C. An, A. Campbell, X. Zhou, "Hilight: hiding bits in pixel translucency changes", *In Proc. of the 1st ACM MobiCom Workshop on Visible Light Communication Systems (VLCS)*, pp. 45 - 50, 2014.

[8] R. Carvalho, C.-H. Chu, and L.-J. Chen., "IVC: Imperceptible video communication", *The 15th International Workshop on Mobile Computing Systems and Applications (Demo)*, 2014.

[9] T. Li, C. An, X. Xiao, A. Campbell, and X.Zhou, "Real-Time Screen-Camera Communication Behind Any Scene", *In Proceedings of the 13th ACM Annual International Conference on Mobile Systems*, pp. 197 - 211, 2015.

[10] E. Wengrowski, K. Dana, M. Gruteser, and N. Mandayamy, "Reading Between the Pixels: Photographic Steganography for Camera Display Messaging", *International IEEE Conference on Computational Photography*, pp. 1 - 11, 2017.

[11] W. Du, J. C. Liando, M. Li, "Soft Hint Enabled Adaptive Visible Light Communication over Screen-Camera Links", *IEEE Transactions on Mobile Computing*, pp. 527 - 537, 2016.

[12] T. Hao, R. Zhou, G. Xing, "COBRA:Color Barcode Streaming for Smartphone Systems", *In Proceedings of the 10th ACM international conference on Mobile systems, applications, and services*, pp. 85 - 98, 2012.

[13] W. Hu, J. Mao, Z. Huang, Y. Xue, J. She, K. Bian, and G. Shen, "Strata: Layered coding for scalable visual communication", *In Proceedings of the 20th ACM Annual International Conference on Mobile Computing and Networking*, pp. 79 - 90, 2014.

[14] W. S. Geisler, J. S. Perry, "Real-time foveated multiresolution system for low-bandwidth video communication", *In Proceedings SPIE Volume 3299, Human Vision and Electronic Imaging III*, 1998

[15] H.R. Wu, K.R. Rao, "Digital Video Image Quality and Perceptual Coding 1st Edition", ch14, 2005.

[16] J. S. Lee, F. D. Simone, and T. Ebrahimi, "Subjective Quality Evaluation of Foveated Video Coding Using Audio-Visual Focus of Attention", *IEEE Journal of Selected Topics in Signal Processing*, pp. 1322 - 1331, 2011.

[17] J. Hrault, B. Durette, "Modeling Visual Perception for Image Processing, Computational and Ambient Intelligence IWANN", *Lecture Notes in Computer Science*, vol. 4507, pp. 662 - 675, 2007.

[18] K. Parrish, "Nvidia plans to prove that new method improves image quality in virtual reality", July 22,2016, [Online], Avaliable: www.digitaltrends.com/virtual-reality/nvidia-research-foveated-rendering-vr-smi/, [Accessed:Feb. 12,2018].

[19] Andrew B. Watson, "A formula for human retinal ganglion cell receptive field density as a function of visual field location", *Journal of vision*, vol. 14, no. 7, 2014.

[20] A. Wang, Z. Li, C. Peng, G. Shen, G. Fang and B. Zeng, "InFrame++:Achieve Simultaneous Screen-Human Viewing and Hidden Screen-Camera Communication", *In Proceedings of the 13th ACM Annual International Conference on Mobile Systems, Applications and Services*, pp. 181 - 195, 2015.

[21] S. Huang, "Backlight modulation circuit having rough and fine illumination signal processing circuit", US20090096742 A1 *US Patent*, Apr. 16 2009.

[22] David L. MacAdam, "Specification of Small Chromaticity Differences", *Journal of the Optical Society of American*, vol. 33, pp. 18-26, 1943.

[23] A. Bokani et al., "Predicting the region of interest for dynamic foveated streaming", *Proc. of International Telecommunication Networks and Applications Conference (ITNAC)*, pp. 137-142, 2015.

[24] B. Dickson, "Unlocking the potential of eye tracking technology", 2017, [Online], Avaliable:https://techcrunch.com/2017/02/19/unlocking-the-potential-of-eye-tracking-technology/, [Accessed: Feb.12,2018].

[25] B. KELLER, " Optical transmission method of data via modulation of display backlighting, in particular in medical technology devices", PCT/EP2014/061609, *EPO Patent Application*, June 2014.

[26] L. U. Khan, "Visible Light Communication: Applications, architecture, standardization and research challenges," *Elsevier, Digital Communications and Networks 3*, pp. 78-88, 2017.

[27] Kolb H et al., "Webvisionthe organization of the retina and visual system", 2013, [Online] Avaliable: http://webvision.med.utah.edu/book/part-i-foundations/simple-anatomy-of-the-retina/. [Accessed: 12 February 2018]

[28] A. Artusi, F. Banterle, K. Debattista, A. Chalmers, "Advanced High Dynamic Range Imaging, Second Edition", *New York: A K Peters/CRC Press*, 2017.

[29] Richard L. Gregory, "Eye and Brain, Third Edition", *McGraw-Hill Paperbacks*, 1978.

[30] Rolf R. Hainich, O. Bimber, "Displays Fundamentals & Applications", *Taylor and Francis Group*, 2011.

[31] M. Bass et al., "Handbook of Optics, Volume I, Fundamentals, Techniques and Design, Second Edition", 1995.

[32] The-Crankshaft Publishing, "Visual System (sensory System) Part 3", 2014, [Online] Avaliable:http://what-when-how.com/neuroscience/visual-system-sensory-system-part-3/, [Accessed: 02 May 2018]

[33] A. Ashok et al., "Characterizing multiplexing and diversity in Visual MIMO", *Proc. of The IEEE 45th Annual Conference on Information Sciences and Systems (CISS)*, pp. 1-6, 2011.

[34] M. A. Hossain, A. Islam and Y. M. Jangf, "Effects of viewing angle between camera and display in invisible image sensor communication", *International IEEE Conference on Information and Communication Technology Convergence (ICTC)*, pp. 1221-1223, 2016.

[35] W. Yuan, K. Dana et al., "Computer vision methods for visual MIMO optical system", *IEEE Computer Society Conference on Computer Vision and Pattern Recognition Workshops (CVPRW)*, pp. 37-43, 2011.

[36] E. Wengrowski, W. Yuan et al., "Optimal radiometric calibration for camera-display communication", *IEEE Winter Conference on Applications of Computer Vision (WACV)*, pp. 1-10, 2016.

[37] Z.Wang and A. C. Bovik, "Embedded foveation image coding, *IEEE Transactions on Image Processing*, vol. 10, no. 10, pp. 1397-1410, 2001.

[38] A. Ashok et al., "Capacity of pervasive camera based communication under perspective distortions", *Proc. of The IEEE International Conference on Pervasive Computing and Communications*, pp. 112-120, 2014.

[39] VIRIBRIGHT, "Comparing LED vs CFL vs Incandescent Light Bulbs", 2018, [Online] Avaliable:https://www.viribright.com/lumen-output-comparing-led-vs-cfl-vs-incandescent-wattage/, [Accessed: 08 May 2018].

[40] G. Cossu et al., "5.6 Gbit/s downlink and 1.5 Gbit/s uplink optical wireless transmission at indoor distances (1.5 m)", *IEEE European Conference on Optical Communication*, pp. 1-3, 2014.

[41] Z. Minglun, Z. Peng and J. Yinjie, "A 5.7 Km Visible Light Communications experiment demonstration", *Proc. of The IEEE Seventh International Conference on Ubiquitous and Future Networks*, pp. 58-60, 2015.

[42] D. Cade, R.Sanyal, "Panasonic unveils 'industry-first' 8K organic image sensor with global shutter", 2018, [Online], Avaliable:https://www.dpreview.com/news/1440456457/panasonic-unveils-industry-first-8k-organic-image-sensor-with-global-shutter, [Accessed: 11 May 2018].

[43] C.F. Lai et al., "DLNA-Based Multimedia Sharing System for OSGI Framework With Extension to P2P Network", *IEEE Systems Journal*, vol. 4, no. 2, pp. 262-270, 2010.

[44] S.C. Liu et al., "A broadband P2P MoD system: Its implementation and application, *In proc. of 11th IEEE International Conference on Parallel and Distributed Systems*, pp. 85-90, 2005.

[45] DLNA 4.0 Transforms Connected Home Experience, 2016, [Online], Available:https://newdlna.squarespace.com/news/2016/6/28/dlna-40-transforms-connected-home-experience-1, [Accessed: 11 May 2018].

[46] DLNA Fulfils Mission, Dissolves as Non-Profit Trade Association, 2017, [Online], Available:https://www.dlna.org/about/organization/, [Accessed: 11 May 2018].

[47] M. Ebling and R. Caceres, "Bar codes everywhere you look", *IEEE Pervasive Computing*, no. 2, pp. 4-5, 2010.

[48] W. Hu, H. Gu and Q. Pu, "LightSync: Unsynchronized Visual Communication over Screen-Camera Links", *ACM Proceedings of the 19th annual international conference on Mobile computing & networking*, pp. 15-36, 2013.

[49] T. Hao, R. Zhou, and G. Xing, "COBRA: color barcode streaming for smartphone systems", *In ACM Proceedings of the 10th international conference on Mobile systems, applications, and services*, pp. 85-98, 2012.

[50] L. Francis, G. Hancke et al., "Practical NFC peer-to-peer relay attack using mobile phones", *ACM Proceedings of the 6th international conference on Radio frequency identification: security and privacy issues*, pp. 35-49, Istanbul, TURKEY, 2010.

[51] M. Allah, "Strengths and weaknesses of near field communication (NFC) technology", *GJCST*, vol. 11, no. 3, 2011.

VITA

Özgür Yıldız is born in 1989, in Afyonkarahisar, TURKEY. He has received his B.Sc degree from Electrical and Electronics Engineering Department of Dokuz Eylül University in 2013. He has been working at VESTEL as system design specialist since 2013. His current research interests are wireless optical communication systems, computer vision and digital image processing.